

## Original Research Article

# Soluble curcumin prepared by solid dispersion using four different carriers: Phase solubility, molecular modelling and physicochemical characterization

Mohamed J Muthu, K Kavitha\*, Karthikeyini S Chitra, S Nandhineeswari

Department of Pharmaceutical Technology, BIT Campus, Anna University, Tiruchirappalli 620024, Tamil Nadu, India

\*For correspondence: **Email:** kavithaaut@gmail.com; **Tel:** +91-9841954918; **Fax:** 0431-2407999

Sent for review: 11 March 2019

Revised accepted: 29 July 2019

### Abstract

**Purpose:** To prepare curcumin solid dispersions (SDs) using four different carriers, evaluate their thermodynamic properties, and carry out physicochemical characterization on them.

**Methods:** Solid dispersions (SDs) of curcumin were prepared using hot melt method. Hydrophilic carriers, including poloxamers (P-407 and P-188), gelucire 50/13 and mannitol were used in the ratios of 1:3, 1:4, 1:5, 1:6 and 1:7 (curcumin : carrier). The new formulations were characterized in the liquid state by phase solubility studies (PSS), and in the solid state using Fourier transform infrared (FTIR) spectroscopy, powder x-ray diffraction (PXRD), differential scanning calorimetry (DSC), thermogravimetric analysis (TGA) and scanning electron microscopy (SEM). Molecular modelling (MM) was also performed on the SDs.

**Results:** The results of PSS revealed an AL-type phase-solubility profile with spontaneous binding process, indicating 1:1 stoichiometry. The stability constant ( $K_a$ ) of curcumin with various carriers at 25 and 37 °C were in the order: P-407 ( $631.9$  and  $524.9 M^{-1}$ ) > P-188 ( $436.48$  and  $388.28 M^{-1}$ ) > gelucire ( $100.14$  and  $112.05 M^{-1}$ ) > mannitol ( $10.88$  and  $11.90 M^{-1}$ ). The maximum stability constants of P-407 at 25 and 37 °C were  $631$  and  $524 M^{-1}$ , respectively, which produced an accurate fit on MM (in silico model). Curcumin-P-407 complex produced enhanced solubility property ( $318 \pm 14.46$ -fold). Physicochemical characterization revealed a shift in curcumin structure from crystalline to amorphous form without any chemical alterations, thereby enhancing solubility.

**Conclusion:** These results shown that the solubility of curcumin is greatly improved after its complexation with P-407 in SD, and the drug is converted into amorphous form without significant chemical modification.

**Keywords:** Curcumin, Carrier, Phase solubility, Molecular modelling, Physicochemical characterization

This is an Open Access article that uses a fund-ing model which does not charge readers or their institutions for access and distributed under the terms of the Creative Commons Attribution License (<http://creativecommons.org/licenses/by/4.0>) and the Budapest Open Access Initiative (<http://www.budapestopenaccessinitiative.org/read>), which permit unrestricted use, distribution, and reproduction in any medium, provided the original work is properly credited.

Tropical Journal of Pharmaceutical Research is indexed by Science Citation Index (SciSearch), Scopus, International Pharmaceutical Abstract, Chemical Abstracts, Embase, Index Copernicus, EBSCO, African Index Medicus, JournalSeek, Journal Citation Reports/Science Edition, Directory of Open Access Journals (DOAJ), African Journal Online, Bioline International, Open-J-Gate and Pharmacy Abstracts

## INTRODUCTION

Enhancement of the solubility of insoluble drugs is a present-day challenge for researchers in the field of pharmaceutical technology. Method-

ologies that improve physicochemical characteristics of compounds include nanosizing, micronization, upgrade of wettability of powders and contact angle, and the approach of liposomes and SD [1].

Curcumin is classified under Biopharmaceutics Classification System (BCS) as a class-IV compound because of its poor water solubility (> 0.1 mg/ml at 25 °C in aqueous buffer), and low permeability via intestinal epithelial cells. Despite its therapeutic effectiveness, the clinical use of curcumin is limited due to poor water solubility, slow absorption in the gastrointestinal tract (GIT), and low bioavailability. Curcumin exhibits a wide range of pharmacological activities, and induces apoptosis in many cellular systems [2]. Toxicological studies have shown that curcumin is non-toxic even at very high concentrations. The aim of this study was to prepare curcumin SDs using four different carriers, subject them to physicochemical characterization, and evaluate their thermodynamic properties.

## EXPERIMENTAL

### Materials

The reagents and chemicals used in this study were of analytical grade. Gelucire 50/13 was provided by Gattefosse Pvt. Ltd. (India); curcumin (99 % pure) was obtained from Sisco Research Laboratories Pvt. Ltd. (India), while poloxamers (P-407 and P-188) were products of BASF Corporation (India). Mannitol was purchased from SD Fine-Chem Pvt Ltd. (India).

### Phase solubility studies (PSS)

Phase solubility was performed using standard methods [3]. Excess amount of curcumin was added to aqueous solutions of each carrier (P-407, P-188, gelucire and mannitol) containing increasing concentrations of the individual carrier (1 - 15 % w/v). The flasks were maintained at 25 °C for 24 h with continuous stirring at intervals of 30 min using a magnetic stirrer. The saturated solution was sonicated for 20 min. and then centrifuged at 4000 rpm for 10 min. The resultant supernatant was filtered using Millipore membrane filter of 0.45 µm pore size to obtain a filtrate which was suitably diluted and analyzed spectrophotometrically at 425 nm (Agilent Cary 60 UV-Vis Spectrophotometer, USA). The stability complexation constant ( $K_{1:1}$ ) was determined from the slope and intercept of the stage solvency curve, where the intercept is the inherent dissolvability of curcumin.

$$K_{1:1} = \frac{S}{I(1-S)}$$

where S and I represent slope and intercept, respectively.

The change in enthalpy ( $\Delta H$ ) on complexation was determined from Van't Hoff equation as shown below:

$$\ln\left(\frac{k_2}{k_1}\right) = \Delta H \frac{T_2 - T_1}{RT_2T_1}$$

where  $k_2$  and  $k_1$ , and  $T_2$  and  $T_1$  refer to the stability constants and corresponding temperatures in Kelvin at 37 and 25 °C, respectively.

The Gibbs free energy change ( $\Delta G$ ) and entropy ( $\Delta S$ ) on complexation and solubilization were calculated as in Eqs 1 and 2.

$$\Delta G = -RT \ln K \dots\dots\dots (1)$$

where R is the gas constant (R = 8.314 J/mol K)

$$\Delta S = \frac{\Delta H - \Delta G}{\Delta T} \dots\dots\dots (2)$$

### Molecular modelling (MM)

Molecular interactions between curcumin and carriers were determined using BIOVIA discovery studio (2017) platform [4]. Initially, the grid was generated around the carriers (P-407, P-188 and gelucire), and coordinates of X (6.123), Y (4.641) with Z (0.229); and X (10.521), Y (-2.624) with Z (-0.861). Subsequently, ten best conformations were selected for studying the interactions between the carriers and curcumin. The carriers were docked (C-Docker protocol in DS) around the drug, and finally, the stable complex was saved for interaction analysis. CHARMM-based algorithm was used to analyze the interaction between the complexes.

### Preparation of physical mixtures (PM) and solid dispersion (SD)

Physical mixtures (PM) of curcumin and the carriers (poloxamers, gelucire and mannitol) were prepared by mixing accurately weighed amounts of curcumin and carriers in a mortar by simple trituration (curcumin: carrier ratios were 1:1, 1:2 and 1:4). The SD of varying compositions (1:3, 1:4, 1:5, 1:6 and 1:7) were prepared using a melting method by adding curcumin to the molten carrier at 70 °C with continuous stirring at 700 rpm for 15 min until a homogeneous dispersion was obtained. The resultant melt was allowed to solidify, cooled at room temperature (28 °C), pulverized, sieved (150 - 125 µm filter) and stored at 25 °C in a desiccator [5]. Physical control blend of the same composition was prepared using homogenization with mortar and pestle based on the guidelines of geometrical mixing, and then screened.

## Aqueous solubility study

An excess amount of samples (pure curcumin, PM and SD) were added to Milli Q water in a volumetric flask with a steady temperature of  $37 \pm 0.5$  °C for 24 h and shaken in between at 30 min intervals [6]. Subsequently, content filtered through Millipore membrane filter (0.45 $\mu$ m), diluted suitably and UV absorbance was measured.

## Characterization of PM and SD

The difference in structure was analyzed in the solid powder by the KBr disc method done in the wavenumber range of 4000–400  $\text{cm}^{-1}$  with a scan speed of 1  $\text{cm}^{-1}$  in an FTIR spectrophotometer (JASCO/FTIR-6300, Japan). The PXRD patterns of samples were observed with Rigaku Ultima III XRD (Rigaku Co., Ltd., Tokyo, Japan). PXRD was performed through a K $\beta$  filter and Cu Energy at a current of 30 kV and a 15 mA current. The powder samples were reliably spun and examined at a degree of 1°/min over a 2 $\theta$  range of 5– a pre-stacked PC program handled 80° (data are shown at 5–40°) [7]. The DSC thermogram of powdered samples detected with thermal analysis system (DSC; Pyris 6, Diamond TG/DTA; Perkin-Elmer Instruments, USA) underflow (20 mL/min) of nitrogen with 3 mg samples positioned in a sealed aluminum pan. The sample heated in the range of 10 °C/min from 20 to 300 °C [8].

## Morphological evaluation

A thin layer of PM and SD (100 Å) was gold-coated using a sputter coater before amplification at a voltage of 5.0 kV, and then subjected to SEM.

## Statistical analysis

Data are expressed as mean  $\pm$  standard deviation, and the statistical analysis was performed using SPSS (16.0).

**Table 1:** Thermodynamic parameters of curcumin with the carriers at 25 and 37 °C

Carrier	T (°C)	Intercept (mM)	K <sub>a</sub> (M <sup>-1</sup> )	$\Delta G$ (kJ/mol)	$\Delta H$ (kJ/mol)	$\Delta S$ (kJ/mol K) $\times 10^{-3}$
P-407	25	$5.70 \times 10^{-4}$	$631.97 \pm 25.81$	$-15.98 \pm 0.10$	$-11.90 \pm 0.52$	$13.68 \pm 2.00$
	37	$7.80 \times 10^{-4}$	$524.91 \pm 20.81$	$-16.15 \pm 0.02$		
P-F188	25	$2.06 \times 10^{-4}$	$436.48 \pm 17.12$	$-15.06 \pm 0.22$	$-7.50 \pm 0.49$	$25.38 \pm 7.00$
	37	$4.72 \times 10^{-4}$	$388.28 \pm 16.87$	$-15.37 \pm 0.25$		
Gelucire 50/13	25	$2.04 \times 10^{-4}$	$100.14 \pm 6.18$	$-11.41 \pm 0.22$	$7.20 \pm 0.88$	$62.45 \pm 6.00$
	37	$2.12 \times 10^{-4}$	$112.05 \pm 7.12$	$-12.16 \pm 0.26$		
Mannitol	25	$5.97 \times 10^{-5}$	$10.88 \pm 1.44$	$-5.78 \pm 0.08$	$7.35 \pm 0.87$	$43.99 \pm 2.00$
	37	$8.14 \times 10^{-5}$	$11.90 \pm 1.59$	$-6.33 \pm 0.09$		

## RESULTS

### Outcomes of PSS

A standard linear curve was obtained for concentrations of curcumin ranging from  $5.97 \times 10^{-5}$  to  $5.7 \times 10^{-4}$  mM and  $8.14 \times 10^{-5}$  to  $7.8 \times 10^{-4}$  mM at 25 and 37 °C, respectively. The results revealed an A<sub>L</sub>-type phase-solubility profile (Table 1).

Apparent K<sub>1:1</sub> was calculated from the slope and intrinsic intercept of solubility curves acquired by plotting concentration of dissolved curcumin (% w/v) against concentration of the carriers (% w/v) (Figures 1a & 1b). The stability constant (K<sub>a</sub>) of curcumin with various carriers at 25 and 37 °C were in the order: P-407 (631.9 and 524.9 M<sup>-1</sup>) > P-188 (436.48 and 388.28 M<sup>-1</sup>) > gelucire (100.14 and 112.05 M<sup>-1</sup>) > mannitol (10.88 and 11.90 M<sup>-1</sup>). Changes in entropy ( $\Delta S$ ), Gibbs free energy ( $\Delta G$ ) and enthalpy ( $\Delta H$ ) were extrapolated from PS chart. Negative  $\Delta G$  indicated favorable conditions.

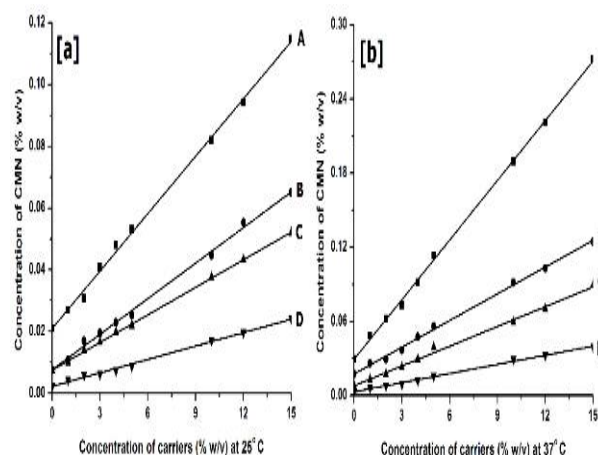


**Figure 1:** Phase solubility diagrams of curcumin. (A) P-407; (B) P-188; (C) GLR; and (D) MNT in water in the presence of the carriers at [a] 25 °C and [b] 37 °C

## Outcomes of MM

Computer modelling of poloxamers and gelucire provided insight into the subtle elements of their atomic structures (Figure 2). The ideal 1:1 curcumin/poloxamer complex was composed of a central hydrophobic polyoxypropylene (polypropylene oxide) chain for enhanced hydrophobic interaction with benzene rings and methyl group of curcumin (Figure 2a). In total, four hydrophobic bonds were formed at a distance range of 4.7 - 5.3 Å. A tighter curcumin/poloxamer cavity fit which accounted for the little changes in enthalpy ( $\Delta H = -11.9$  and  $-7.50$  kJ/mol) and positive changes in entropy ( $\Delta S = 1$  and  $2$  J/mol.K) was observed (Figure 2b). This resulted in the formation of a complex due to enthalpy-entropy compensation.

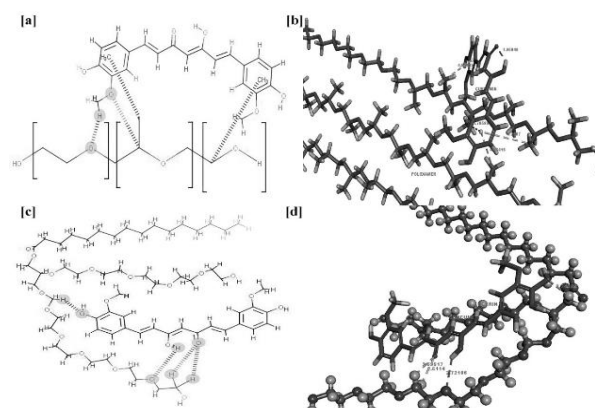


**Figure 2:** Molecular modeling for the 1:1 curcumin/poloxamer complex. (a) 2D illustration of enol form of curcumin monomer showing hydrophobic bonds of phenolic OH group; (b) 3D representation of Dock-pose of enol form of curcumin; (c) 2D illustration of a diketo form of curcumin showing hydrogen bonds of phenolic OH group; and (d) 3D representation of Dock-pose of curcumin (dotted lines indicate most important interactions, and the distances are measured in Å)

An optimal 1:1 ratio complex configuration obtained for neutral curcumin with gelucire, and interaction between the complex showed that OH group of curcumin formed two conventional hydrogen bonds with a bond distance of 2.7 Å, while the C = O group formed two weak hydrogen bonds with a bond distance of 2.5 Å

(Figure 2c). The optimal hydrogen bonds in curcumin/gelucire complex were the complete interaction with ketone group of curcumin at a bond distance of 2.59 Å (Figure 2d). Thus, gelucire has a high tendency for complexation ( $K_{1:1} = 100$  and  $112$  at  $25$  and  $37$  °C, respectively) (Table 1). Subsequently, the formation of a stable and soluble complex accounted for the significant changes in enthalpy ( $\Delta H = 7.2$  kJ/mol), and positive changes in entropy ( $\Delta S = 6$  J/mol K).

## Aqueous solubility

The aqueous solubility of pure curcumin at  $37$  °C after 24 h was 0.04 mg/ml. The solubility of curcumin SD (1:3 to 1:7) was enhanced by 270-322 and 169-195 folds with P-407 and P-188, respectively, due to strong surface active property which made curcumin molecules to be well adsorbed by the carriers. Aqueous solubility of gelucire binary system showed 121 to 144-fold enhancement of solubility. However, mannitol binary system showed poor enhancement of solubility (16-23 folds). These results are shown in Table 2.

## FTIR spectra

The FTIR spectra of pure curcumin, carriers, PM and SD are shown in Figures 3a & 3b. Curcumin OH group exhibited stretch vibrations at  $3324.68$  and  $3015.16$   $\text{cm}^{-1}$ , which peaked at  $1742.37$  and  $1629.55$   $\text{cm}^{-1}$ . However, the carbonyl group in its structure peaked at  $1597.73$  and  $1507.1$   $\text{cm}^{-1}$ . The presence of C - H stretch (alkanes), C - C stretch (in the ring), and aromatic ring were evident from the traces. Characteristic bands of P-407 and P-188 were observed at  $3479.92$ ,  $2974.66$ ,  $1636.30$ ,  $957$   $\text{cm}^{-1}$  and  $3497.27$ ,  $2889.80$ ,  $1641.13$  and  $955.55$   $\text{cm}^{-1}$  which matched with O - H stretching, C - H stretching, C - O stretching and C - H bending vibrations. In gelucire, peaks at  $3269.72$ ,  $2915.84$ ,  $1730.80$ ,  $1465.63$  and  $719.31$   $\text{cm}^{-1}$  corresponding to O - H stretching (alcohol), C - H stretching ( $sp^3$ ), C - O stretching, C - C stretching and C - H bending vibrations of reduced intensity were observed in the SD and PM.

**Table 2:** Aqueous-solubility data of curcumin SD

Curcumin: carrier ratio	Aqueous solubility ( $\times 10^{-1}$ , mg/ml)					
	1:3	1:4	1:5	1:6	1:7	
Pure curcumin at $37$ °C		0.04 $\pm$ 0.00				
P-407	10.81 $\pm$ 0.22	11.10 $\pm$ 0.16	12.10 $\pm$ 0.24	12.50 $\pm$ 0.23	12.90 $\pm$ 0.26	
P-F188	6.79 $\pm$ 0.28	7.02 $\pm$ 0.16	7.42 $\pm$ 0.24	7.60 $\pm$ 0.22	7.80 $\pm$ 0.26	
Gelucire 50/13	4.87 $\pm$ 0.28	4.92 $\pm$ 0.16	5.29 $\pm$ 0.24	5.53 $\pm$ 0.25	5.79 $\pm$ 0.24	
Mannitol	0.67 $\pm$ 0.28	0.70 $\pm$ 0.25	0.80 $\pm$ 0.22	0.81 $\pm$ 0.32	0.91 $\pm$ 0.34	

The characteristic bands of mannitol were observed at 3398.92, 2969.84, 2701.78, 2513.76, 1744.30 and 962.30  $\text{cm}^{-1}$ , indicative of O - H stretching (alcohol), C - H stretching, O - H stretching (carboxylic acid), S - H (thiol) stretching, C - O stretching and C - H bending vibrations. In the case of curcumin-mannitol PM and SD, O - H stretching vibrations were exhibited dominantly with reduced intensity (Figure 3b), while C - H stretching vibration response in mannitol was demonstrated both in the PM and SD.

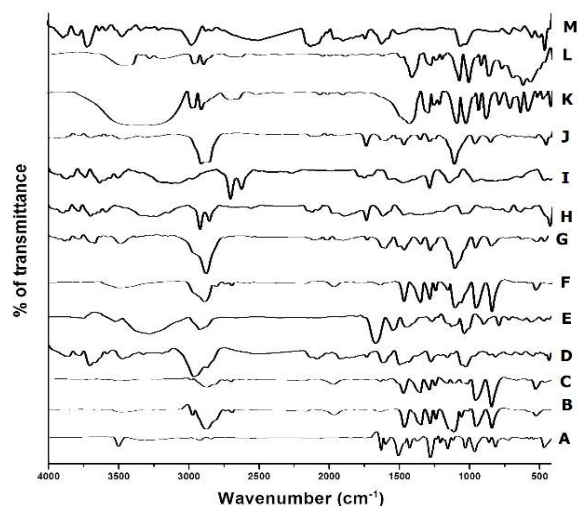


**Figure 3:** FTIR spectra of samples. (A) Curcumin; (B) P-407; (C) curcumin-P-407 (PM); (D) curcumin-P-407 (SD); (E) P-F188; (F) curcumin-P-F188 (PM); (G) curcumin-P-F188 (SD); (H) gelucire; (I) curcumin-gelucire (PM); (J) curcumin-gelucire (SD); (K) mannitol; (L) curcumin-mannitol (PM); and (M) curcumin-mannitol (SD)

### Crystalline properties

The PXRD patterns of curcumin, carriers, PM and SD are shown in Figures 4a & 4b. Curcumin exhibited sharp peaks at diffraction angle ( $2\theta$ ) of  $8.98^\circ$  and  $17.38^\circ$  (indicative of presence of a crystalline form of the drug), and many tiny peaks at  $23.48^\circ$ ,  $24.72^\circ$ ,  $25.68^\circ$ ,  $26.22^\circ$  and  $27.50^\circ$ . The peaks of P-407 ( $2\theta$  of  $19.26^\circ$  and  $23.00^\circ$ ) and P-188 ( $2\theta$  of  $19.24^\circ$  and  $23.32^\circ$ ) indicated crystalline domain of an amorphous polymeric material. Mannitol exhibited many diffraction peaks with high intensity at  $2\theta$  of  $18.96^\circ$ ,  $21.00^\circ$  and  $23.54^\circ$ , indicative of crystalline pattern. However, gelucire exhibited amorphous characteristics due to lack of complete stereo-uniformity and presence of a large lateral group in the carrier.

In Figure 4b, the PM and SD of curcumin-gelucire exhibited peaks with reduced intensity at diffraction  $2\theta$  of  $8.98^\circ$  and  $17.38^\circ$ , when compared with that of crystalline curcumin. The

amorphous nature of the carrier was replicated in its SD as revealed by the respective diffractograms. The X-ray chart of mannitol revealed the same diffraction pattern observed in its PM producing peak at a diffraction angle ( $2\theta$ ) of  $9.28^\circ$  found in the SD.

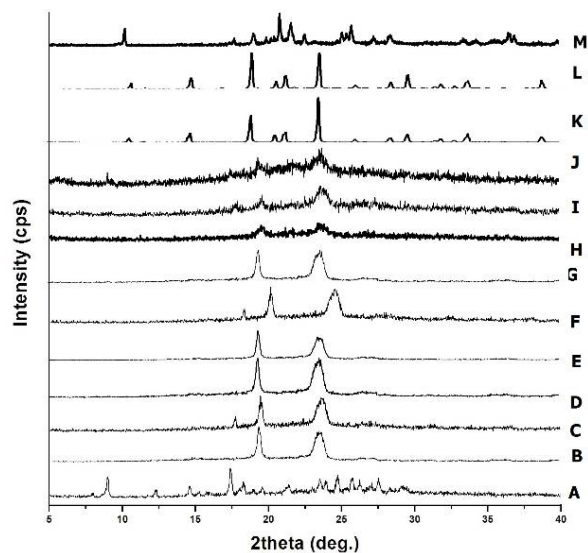


**Figure 4:** PXRD pattern of samples. (A) Curcumin; (B) P-407; (C) curcumin-P-407 (PM); (D) curcumin-P-407 (SD); (E) P-F188; (F) curcumin-P-F188 (PM); (G) curcumin-P-F188 (SD); (H) gelucire; (I) curcumin-gelucire (PM); (J) curcumin-gelucire (SD); (K) mannitol; (L) curcumin-mannitol (PM); and (M) curcumin-mannitol (SD)

### Thermal properties

The thermograms of curcumin, P-407, P-188, gelucire, the corresponding PM and SD are shown in Figure 5b. Thermograms of curcumin ( $179.8^\circ\text{C}$ ), P-407 ( $52.8^\circ\text{C}$ ), P-188 ( $53.1^\circ\text{C}$ ) and gelucire ( $49.7^\circ\text{C}$ ) exhibited sharp endothermic peaks.

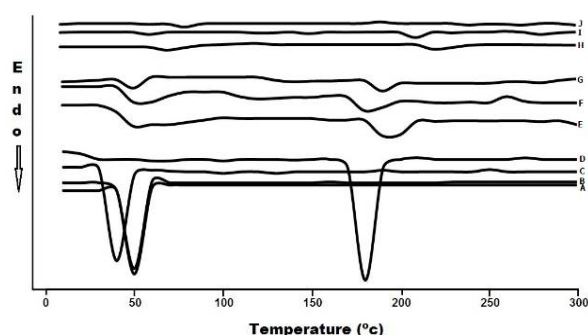


**Figure 5:** Thermograms of SD. (A) P-F188; (B) P-407; (C) GLR; (D) Pure curcumin; (E) curcumin-gelucire PM (1:7); (F) curcumin-P-F188 PM (1:5); (G) curcumin-P-407 PM (1:6); (H) curcumin-gelucire SD (1:7); (I) curcumin-PF188 SD (1:5); and (J) curcumin-P-407 SD (1:5)

## Morphological properties of SDs

As shown in Figure 6, curcumin appeared as a characteristic prism-shaped crystal with mean PS of 15  $\mu\text{m}$ , while P-407 appeared as smooth-surfaced particles with mean PS of 50  $\mu\text{m}$ .

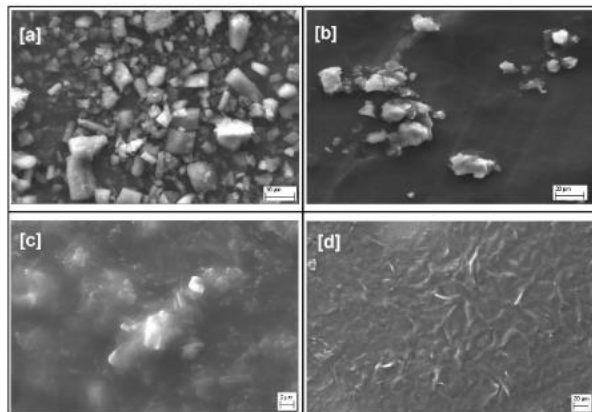


**Figure 6:** Scanning electron micrographs of samples as revealed by SEM. (a) Curcumin; (b) P-407; (c) curcumin-P-407 PM; and (d) curcumin-P-407 SD

## DISCUSSION

In the present study, curcumin SDs were prepared using four different carriers, and their thermodynamic properties and physicochemical characteristics were determined. The results of PSS revealed an  $A_L$ -type phase-solubility profile, and are in agreement with those reported previously [9]. Molecular modelling showed that a total of four hydrophobic bonds were formed at a distance range of 4.7 - 5.3  $\text{\AA}$ . A tighter curcumin/poloxamer cavity fit which accounted for the little changes in enthalpy and positive changes in entropy was observed. These results are consistent with those reported in previous studies [10]. The solubility of curcumin SD was greatly enhanced with P-407 and P-188, probably due to strong surface active property which made curcumin molecules to be well adsorbed by the carriers [11].

The results from FTIR analysis showed that curcumin OH group exhibited stretch vibrations suggestive of the presence of two hydroxyl groups. This result is in agreement with previous reports [12]. Characteristic bands of P-407 and P-188 suggested O - H stretching, C - H stretching, C - O stretching and C - H bending vibrations. Gelucire peaks were suggestive of O - H stretching (alcohol), C - H stretching ( $Sp^3$ ), C - O stretching, C - C stretching and C - H bending vibrations of reduced intensity in the SD and PM [13]. The characteristic bands of mannitol were suggestive of O - H stretching (alcohol), C - H stretching, O - H stretching (carboxylic acid), S -

H (thiol) stretching, C - O stretching and C - H bending vibrations. In curcumin-mannitol PM and SD, O - H stretching vibrations were exhibited dominantly with reduced intensity, while C - H stretching vibration response to mannitol was demonstrated both in the PM and SD. Curcumin peak due to C = O group was an indication of hydrogen bond interaction.

The PXRD patterns of curcumin exhibited sharp peaks indicative of the presence of a crystalline form of the drug. The peaks of P-407 and P-188 at diffraction angle of 19.24° and 23.32° indicated crystalline domain of an amorphous polymeric material. Mannitol exhibited many diffraction peaks with high intensity, suggestive of crystalline pattern [14]. However, gelucire exhibited amorphous characteristics due to lack of complete stereo-uniformity and presence of a large lateral group in the carrier. The PM and SD of curcumin-gelucire exhibited peaks with reduced intensity at diffraction  $2\theta$  of 8.98° and 17.38°, when compared with that of crystalline curcumin. Amorphous nature of the carrier was replicated in SDs as revealed by their respective diffractograms. The thermograms of curcumin, P-407, P-188 and gelucire exhibited sharp endothermic peaks. These results are in agreement with those previously reported [15-17]. The hydrodynamic PS of curcumin-P-407 PM is suggestive of bi-modal size distribution [18].

Phase solubility studies are used to assess the effect of carriers on solubility of drugs. The solubility of curcumin SD was greatly increased, relative to that of the pure compound. The solubility increased with temperature and concentration of carrier. The increased solubility of curcumin SD may be due to changes in hydrophobic and Van der Waals forces between curcumin and the carriers. The slope of the PSS diagram obtained suggested 1:1 complex stoichiometry ratio, and these results are in agreement with those reported previously [19]. Negative  $\Delta G$  values were obtained in all the carriers, and  $\Delta G$  values decreased with increase in molecular weights of the carriers.

These results suggest spontaneity of binding. The calculated  $\Delta H$  values were negative (exothermic) in P-407 and P-188 complexes, except for the solubility system with gelucire and mannitol. Similarly, the  $\Delta S$  in curcumin-gelucire and curcumin-mannitol systems were marginally high, indicative of an endothermic reaction [20]. The very strong binding constant of poloxamer is due to the polyoxyethylene-polypropylene block copolymer nonionic surfactant which has a hydrophile-lipophile balance (HLB) value of 18-

23. Polypropylene oxide (PPO) for the most part, forms a focal hydrophobic center wherein methyl groups associate with curcumin undergoing solubilization via Van der Waals interactions [21].

However, solubility due to polyoxyethylene oxide (PEO) is blocked by hydrogen bonding between oxygen and water molecules. Endothermic process (+ $\Delta H$ ) of binding with high positive  $\Delta S$  of gelucire enhanced wettability, while being surrounded with a hydrophilic matrix, via the reduction of interfacial tension between curcumin and water. The solubility of curcumin increased with increase in concentration, suggesting the solvent properties of gelucire for curcumin. An exception was noticed with mannitol where high positive  $\Delta S$  was obtained due to ionization of ligand and water molecules, indicative of an endothermic binding process. Spontaneity of reaction due to negative  $\Delta G$  means least complex formation between mannitol and curcumin. These results support the formation of a soluble complex between carriers and lipophilic curcumin.

*In silico* studies established better interaction between curcumin and poloxamer than between curcumin and gelucire. Molecular modelling data supported the results of phase solubility measurement.

Surface property of a surfactant improves its wetting characteristics by decreasing the surface tension of vehicle used so that drug molecules are entrapped within the aqueous environment. In this study, aqueous solubility of curcumin in the SD was enhanced regardless of the concentration of carrier. Aqueous solubility of gelucire binary system was greatly enhanced due probably to formation of many hydrogen bonds between water molecules and oxygen atoms of electron-rich gelucire chain. However, mannitol binary system showed minimal enhancement of solubility due probably to formation of few hydrogen bonds between water and curcumin molecules. These results are in agreement with those reported previously [22].

Photomicrographs of curcumin SD on SEM revealed topological changes which were uniform and homogeneously dispersed at the molecular level. Curcumin on complexation with P-407 was completely converted to the amorphous form. Functionalized dye test without auxiliaries showed that curcumin-P-407 exhibited enhanced dyeing effect, an indication that the solubility of curcumin increased more evenly in water on complexation with P-407. These results are consistent with those of previous reports [23].

## CONCLUSION

The results obtained in this study demonstrate that the solubility of curcumin is greatly improved after its complexation with P-407 in SD, and the drug is converted into amorphous form without significant chemical modification. The soluble curcumin enhances its potential activity and is devoid of the insoluble drug drawbacks. We hope the present investigation will inspire further influences along these lines.

## DECLARATIONS

### Acknowledgement

The authors wish to specially thank Prof. K. Ruckmani, Department of Pharmaceutical Technology, Anna University, Tiruchirappalli and Prof. S. Shanmuganathan, Department of Pharmacy, Sri Ramachandra University, Chennai, for their immense support for this work.

### Conflict of interest

No conflict of interest is associated with this work.

### Contribution of authors

This work was done by the authors named in this article and all liabilities pertaining to claims relating to the content will be borne by them.

### Open Access

This is an Open Access article that uses a funding model which does not charge readers or their institutions for access and distributed under the terms of the Creative Commons Attribution License (<http://creativecommons.org/licenses/by/4.0>) and the Budapest Open Access Initiative (<http://www.budapestopenaccessinitiative.org/read>), which permit unrestricted use, distribution, and reproduction in any medium, provided the original work is properly credited.

## REFERENCES

1. Bansal SS, Goel M, Aqil F, Vadhanam MV, Gupta RC. Advanced drug delivery systems of curcumin for cancer chemoprevention. *Cancer Prev Res*. 2011; 4: 1158-1171.
2. Alberto F, Valeria Z, Antonio M, Francesca C, Anna VM. Mediterranean diet and colorectal cancer: A systematic review. *Nutrition*. 2017; 43: 83-88.
3. Higuchi T, Connors KA. Phase-solubility techniques. *Adv Anal Chem Instrum*. 1965; 4: 117-212.

4. Camelia N, Corina A, Angela N, Crina-Maria M. Phase solubility studies of the complexes of repaglinide with  $\beta$ -cyclodextrin and  $\beta$ -cyclodextrin derivatives. *FARMACIA*. 2010; 58: 620-628.
5. Fernandes CM, Vieira MT, Veiga FJB. Physicochemical characterization and in vitro dissolution behavior of nicardipine-cyclodextrins compounds. *Eur J Pharm Sci*. 2002; 15: 79-88.
6. Chutimaworapan S, Oguchi G, Ritthidej C, Yamamoto K, Yonemochi E. Effect of water-soluble carriers on dissolution characteristics of nifedipine solid dispersions. *Drug Dev Ind Pharm*. 2000; 26: 1141-1150.
7. Veenus ST, Linda JKH, Narra K, Selvamani P, Lalhlenmawia H, Thanzami K, Laldusanga P, Ruckmani K. Exploitation of novel gum *Prunus cerasoides* as muco-adhesive beads for a controlled release drug delivery. *Int J Biomed*. 2016; 85: 667-673.
8. Subramanian N, Kumar PS, Chandrasekar P, Rajaguru P, Sivakumar M, Ruckmani K. Co-encapsulated resveratrol and quercetin in chitosan and peg modified chitosan nanoparticles for efficient intraocular pressure reduction. *Int J Biomed*. 2017; 104: 1837-1845.
9. Le HT, Jeon HM, Lim CW, Kim TW. Synthesis, cytotoxicity and phase-solubility study of cyclodextrin click clusters. *J Pharm Sci*. 2014; 103: 3183-3189.
10. Gangurde AB, Kundaikar HS, Javeer SD, Jaiswar DR, Degani MS, Amin PD. Enhanced solubility and dissolution of curcumin by a hydrophilic polymer solid dispersion and its *In-silico* molecular modeling studies. *J Drug Deliv Sci Tech*. 2015; 29: 226-237.
11. Eunmi B, Mijung P, Seonghee J, Taekhyun K, Eun-Hee K, Kiwon J, Kim A. Poloxamer-based thermoreversible gel for topical delivery of emodin: influence of P407 and P188 on solubility of emodin and its application in cellular activity screening. *Molecules*. 2017; 22: 1-10.
12. Kurniawansyah F, Quachie L, Mammucari RF, Neil R. Improving the dissolution properties of curcumin using dense gas antisolvent technology. *Int J Pharm*. 2017; 521: 239-248.
13. El-Badry M, Fetih G, Fathy M. Improvement of solubility and dissolution rate of indomethacin by solid dispersions in gelucire 50/13 and PEG4000. *Saud Pharm J*. 2009; 17: 217-225.
14. Jang OJ, Kim ST, Lee K, Oh E. Improved bioavailability and antiasthmatic efficacy of poorly soluble curcumin solid dispersion granules obtained using fluid bed granulation. *Bio Med Mat Eng*. 2014; 24: 413-429.
15. Juskenas R, Karpavicienė V, Pakstas V, Selskis A, Kapočius V. Electrochemical and XRD studies of Cu-Zn coatings electrodeposited in solution with d-mannitol. *J Electroanal Chem*. 2007; 602: 237-244.
16. Fini A, Moyano JR, Gine JM, Perez-Martinez JI, Rabasco AM. Diclofenac salts solid dispersions in PEG 6000 and gelucire 50/13. *Eur J Pharm Biopharm*. 2005; 60: 99-111.
17. Chen Z, Xia Y, Liao S, Huang Y, Li Y, He Y, Tong Z, Bin-Li B. Thermal degradation kinetics study of curcumin with nonlinear methods. *Food Chem*. 2014; 155: 81-86.
18. Senthil-Kumar C, Ayyavu M, Antoniraj MG, Vaidevi S, Ruckmani K. Ultrafast synthesis of stabilized gold nanoparticles using aqueous fruit extract of *Limonia acidissima* L and conjugated epirubicin: Targeted drug delivery for treatment of breast cancer. *RSC Adv*. 2016; 32: 26874-26882.
19. Iacovino R, Caso JV, Rapuano F, Isidori ARM, Lavorgna M, Malgieri G, Isernia C. Physicochemical characterization and cytotoxic activity evaluation of hydroxymethyl ferrocene:  $\beta$ -cyclodextrin complex. *Molecules*. 2012; 17: 6056-6070.
20. Mahmoud E. Physicochemical characterization and dissolution properties of meloxicam-gelucire 50/13 binary systems. *Sci Pharm*. 2011; 79: 375-386.
21. Cesareo J, Santosa J, Perez-Martínez JM, Gomez-Pantoja E, Moyanoab JR. Enhancement of albendazole dissolution properties using solid dispersions with Gelucire 50/13 and PEG 15000. *J Drug Deliv Sci Tech*. 2017; 42: 261-272.
22. Ban E, Park M, Jeong S, Kwon T, Kim E, Jung K, Kim A. Poloxamer-based thermoreversible gel for topical delivery of emodin: influence of P407 and P188 on solubility of emodin and its application in cellular activity screening. *Molecules*. 2017; 22: 1-10.
23. Xu S, Chen J, Wang B, Yang Y. Sustainable and hydrolysis-free dyeing process for polylactic acid using nonaqueous medium. *ACS Sustain Chem. Eng*. 2015; 3: 1039-1046.